Drug Design, Development and Therapy

Dovepress
Taylor & Francis Group

Open Access Full Text Article

ORIGINAL RESEARCH

Metagenomic Sequencing Combined with Metabolomics to Explore Gut Microbiota and Metabolic Changes in Mice with Acute Myocardial Infarction and the Potential Mechanism of Allicin

Yijie Gao[1], Gaofeng Qin[2], Shichao Liang[3], Jiajie Yin[4], Baofu Wang[1], Hong Jiang[1], Mengru Liu[1], Fangyuan Luo[3], Xianlun Li[1]

[1]National Integrated Traditional and Western Medicine Center for Cardiovascular Disease, China-Japan Friendship Hospital, Beijing, People's Republic of China; [2]Department of Traditional Chinese Medicine, Binzhou Medical University Hospital, Shandong, People's Republic of China; [3]China-Japan Friendship Hospital, Chinese Academy of Medical Sciences and Peking Union Medical College, Beijing, People's Republic of China; [4]Institute of Clinical Medical Sciences, China-Japan Friendship Hospital, Beijing, People's Republic of China

Correspondence: Xianlun Li, Email leexianlun@163.com

Background: Acute myocardial infarction (AMI) is a significant contributor to global morbidity and mortality. Allicin exhibits promising therapeutic potential in AMI as a primary bioactive component derived from garlic; however, its underlying mechanisms remain incompletely elucidated.

Methods: Our study induced AMI in mice by ligating the left coronary artery, and administered allicin orally for 28 days. The cardioprotective effects of allicin treatment were comprehensively assessed using echocardiography, histopathological examinations, intestinal barrier function, and serum inflammatory factors. The potential mechanisms of allicin were elucidated through analysis of metagenomics and serum metabolomics. Network pharmacology (NP) was used to further investigate and validate the possible molecular mechanisms of allicin.

Results: Our findings revealed allicin's capacity to ameliorate cardiac impairments, improve intestinal barrier integrity, and reduce serum IL-18 and IL-1β levels after AMI. Further analysis demonstrated that the administration of allicin has the potential to ameliorate intestinal flora disorder following AMI by modulating the abundance of beneficial bacteria, such as *g_Lactobacillus, g_Prevotella, g_Alistipes*, and *g_Limosilactobacillus*, while reducing the abundance of harmful bacteria *g_Parasutterella*. Additionally, it exhibits the ability to enhance myocardial energy metabolism flexibility through modulating metabolites and key enzymes associated with the fatty acid metabolic pathway. Mechanistically, NP and in vivo experiments indicated that allicin might suppress pyroptosis and reduce inflammatory response via blocked activation of the NF-κB-mediated NLRP3/Caspase-1/GSDMD pathway. Moreover, Spearman correlation analysis suggested a significant association between the allicin-induced alterations in microbiota and metabolites with cardiac function and inflammatory cytokines.

Conclusion: Our study demonstrated that allicin alleviated myocardial injury and reduced inflammatory response by inhibiting the NF-κB-mediated NLRP3/Caspase-1/GSDMD pathway while remodeling microbiota disturbance, improving serum metabolic disorder, and enhancing the intestinal barrier. These research findings offer a novel perspective on the potential therapeutic value of allicin as an adjunctive dietary supplement to conventional treatments for AMI.

Keywords: acute myocardial infarction, allicin, gut microbiota, metabolomics, intestinal barrier, pyroptosis

Introduction

Acute myocardial infarction (AMI) remains the preeminent global healthcare burden and the leading cause of mortality worldwide.[1] Despite the advancements in percutaneous coronary intervention (PCI) and the introduction of novel thrombolytic medications in cardiology that have saved countless lives among AMI patients, the incidence of heart

Received: 5 November 2024
Accepted: 20 January 2025
Published: 3 February 2025

Graphical Abstract

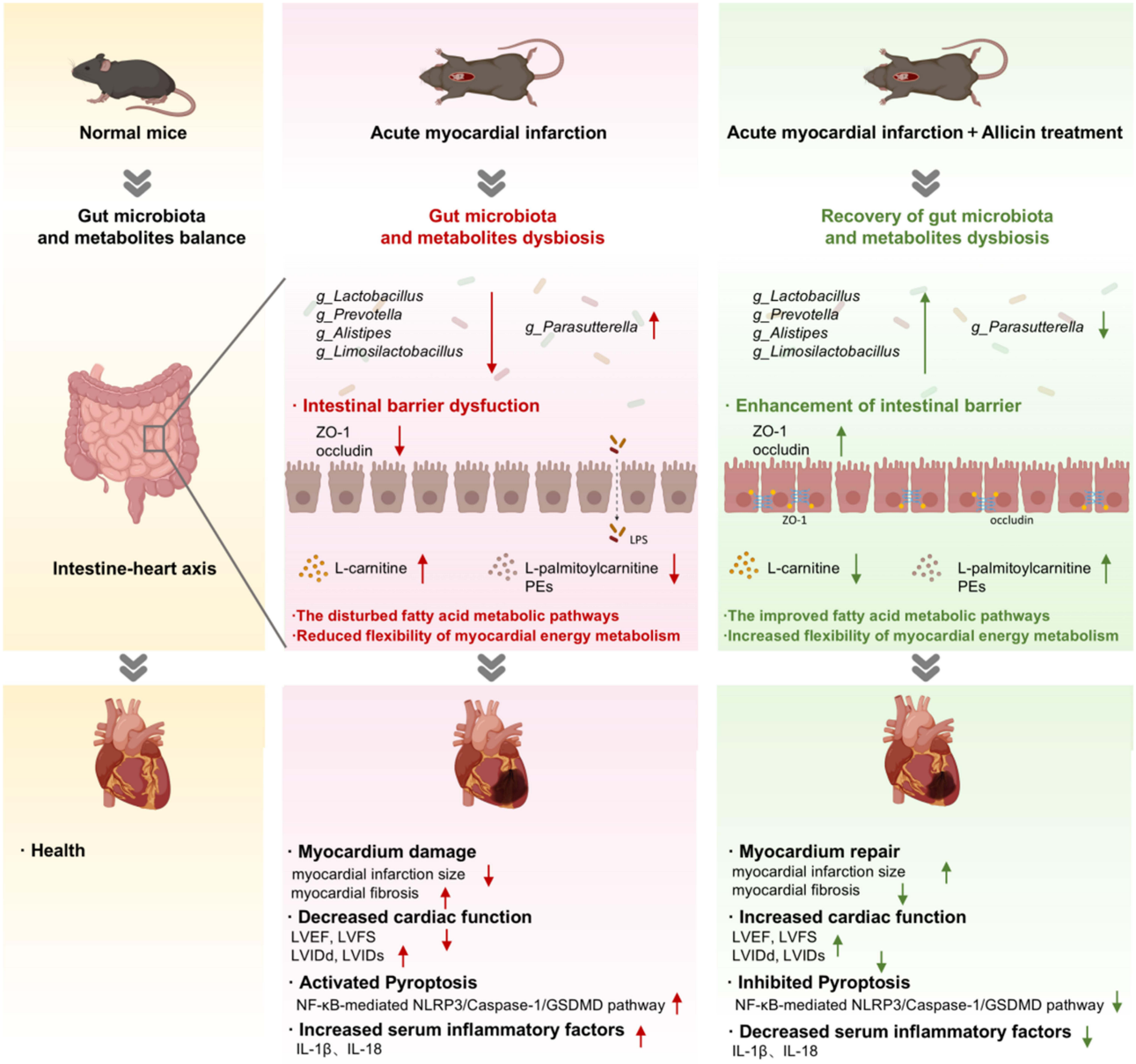

failure (HF) continues to escalate annually.[2] Hence, unveiling the pathogenetic mechanisms and identifying novel therapeutic targets for AMl is imperative.

The etiology and progression of cardiovascular disease (CVD) are influenced by a confluence of factors, including traditional cardiovascular risk factors, metabolic dysregulations, and detrimental lifestyle.[3] In addition, emerging evidence have started to reveal a potential link between CVD and gut microbiota dysbiosis.[4,5] This nascent area of research unveils a new perspective for understanding the potential mechanisms and more comprehensive treatments of AMI. Recent investigations have illuminated the interplay between gut microbiota and AMI severity.[6,7] Studies have documented a correlation between disrupted gut microbial communities' elevated susceptibility to myocardial infarction (MI) and poorer prognoses.[8] This correlation is likely attributed to the impaired left ventricular (LV) function and intestinal hypoperfusion consequent to MI, which induces gut microbiota dysbiosis and augments intestinal permeability

by exacerbating the mucosal injury. This escalation in mucosal damage leads to intensified systemic inflammation and myocardial injury. Therefore, exploring novel therapeutic strategies aimed at remodeling the gut microbiota, fortifying the gut barrier, and reducing systemic inflammation presents a promising avenue for mitigating myocardial damage post-AMI and improving patient outcomes, marking a propitious direction for future AMI prevention and treatment endeavors.

Diet significantly influences human health by modulating the gut microbiome.[9] Recent research underscores that dietary interventions, especially those focusing on heart-healthy diets, can positively impact CVD by altering the gut microbiota and its metabolic outputs, indicating that such interventions may serve as viable treatments for CVD patients.[10] Garlic (*Allium sativum*) enjoys widespread consumption and has been traditionally employed in folk medicine. Numerous studies and epidemiological data have established a robust link between garlic consumption and reducing CVD risk factors.[11] Contemporary research has validated Garlic's potential to exert anti-inflammatory, antilipidemic, antihypertensive, antithrombotic, and antiatherogenic effects,[12,13] leading to its formulation into various herbal health products to enhance cardiovascular wellness. Allicin (diallyl disulfide), an essential bioactive compound in Garlic, is recognized for its multifaceted protective effects on the cardiovascular system, including anti-inflammatory, free radical scavenging, antioxidant, anti-apoptotic, and antimicrobial properties.[14–16] Studies have demonstrated that allicin administration can significantly improve cardiac function and attenuate myocardial injury by reducing myocardial enzyme levels and preserving Ca^{2+} homeostasis post-MI.[17] Moreover, allicin has been shown to alleviate oxidative stress-induced damage and cardiomyocyte apoptosis in MI models by influencing the JNK signaling pathway,[18] underscoring its therapeutic potential for MI. Nonetheless, the precise pharmacological mechanisms of allicin, particularly concerning the gut microbiota and metabolites, are yet to be fully deciphered. These limits impede the development of allicin-based treatments for AMI. Therefore, further investigations are warranted to explore the underlying molecular mechanisms of allicin in treating AMI.

Multi-omics and multi-dimensional analyses have helped enhance our comprehension of disease progression and the mechanisms underlying drug therapeutics. This study explores the impact of allicin on the intestinal barrier integrity, gut microbiota, and serum metabolites following AMI, employing biological analysis, metagenomic sequencing, and untargeted metabolomics analysis. Meanwhile, the potential targets of allicin in the management of AMI were identified using network pharmacology and validated through in vivo experiments to extend the current scientific comprehension of allicin in AMI. We aim to explore regulatory networks for the allicin-mediated treatment of AMI, offering novel strategies for the treatment of AMI.

Materials and Methods

Animals and Medicine

Specific pathogen-free C57BL/6 mice, weighing 20 ± 2 g, were procured from the Beijing Vital River Laboratory Animal Technology Co., Ltd. These mice were maintained in an environment with regulated lighting (12-hour light/dark cycle) and temperature conditions (23 ± 2°C) and were provided unrestricted access to standard chow and water. The animal studies were conducted in strict adherence to the guidelines for the care and use of laboratory animals, as set forth by the US National Institutes of Health (NIH Publication No. 8023, revised 1978), and received approval from the Animal Ethics Committee of the Clinical Research Institute of China-Japan Friendship Hospital (approval number: zryhyy61-03-56).

AMI Model and Drug Administration

Following a three-day acclimatization period, AMI was induced in the mice via surgical occlusion of the left anterior descending coronary artery (LAD). In detail, mice were anesthetized through an intraperitoneal administration of pentobarbital sodium at a dosage of 50 mg/kg. Subsequently, they were intubated and attached to a ventilator (Mouse Ventilator Minivent type 845, Harvard Apparatus). A left thoracotomy was executed between the third and fourth intercostal spaces to expose the heart. The LAD was then securely ligated with a sterile suture approximately 1 mm below the left atrium. Following the ligation, the thoracic cavity was meticulously closed in successive layers. The

successful induction of AMI was verified by observing a pronounced and consistent elevation in the ST segment of the electrocardiogram. Mice in the sham-operated group underwent an identical surgical procedure, excluding the ligation of the LAD.

Animal Grouping and Drug Administration

Following the successful establishment of AMI models, mice were randomly allocated into two distinct cohorts: the model and allicin-treated groups. Allicin, with a catalog number of 539–86-6 and a purity exceeding 98%, was sourced from Shanghai Yuanye Bio-Technology Co., Ltd. (Shanghai, China). Commencing twenty-four hours after the ligation of the LAD coronary artery, mice in the allicin-treated group received daily oral administrations of allicin at a dosage of 20 mg/kg through gavage. Conversely, mice in the model and sham-operated groups were administered an identical volume of distilled water via the same route. All mice were maintained on standard chow for 28 days.

Echocardiography

On the 28th day following the establishment of the AMI model, echocardiographic assessments were performed using a Vevo 3100 animal echocardiography system (VisualSonics, Toronto, Canada). The procedure involved anesthetizing the mice with 1.5% isoflurane, using B-mode ultrasound to examine the thoracic cavity, and transitioning to M-mode ultrasound for acquiring M-mode images and data. Key cardiac function parameters such as ejection fraction (EF), fractional shortening (FS), left ventricular internal end-diastolic diameter (LVIDd), and left ventricular internal end-systolic diameter (LVIDs) were meticulously measured. The acquired data were then analyzed using Vevo Lab offline analysis software (VisualSonics, Toronto, Canada) to assess cardiac function. These measurements were derived from and averaged over three cardiac cycles to ensure accuracy and reliability.

Histological Analysis

Heart and colon tissues were preserved in 4% paraformaldehyde, followed by the preparation of paraffin sections through a sequential process that included dehydration, transparency, wax soaking, embedding, and sectioning. Hematoxylin and eosin (HE) staining was performed to evaluate the histological damage of both heart and colon tissues. Masson's trichrome staining was utilized to assess the specific architecture of cardiac tissue. Images of the stained sections were acquired using a light microscope (Eclipse CI, Nikon Corporation, Tokyo, Japan) to facilitate detailed examination and analysis of tissue morphology.

Biochemistry Assays

Blood samples from mice were allowed to stand at room temperature for 1 hour before being centrifuged at 4°C and 3000g for 15 minutes to separate the serum, which was then stored at −80°C. The concentrations of biochemical markers in the serum, including Interleukin-18 (IL-18) and IL-1β, were quantified using enzyme-linked immunosorbent assay (ELISA) techniques. This involved the use of an IL-18 kit (NeoBioscience, catalog No: EMC011.96, China) and an IL-1β kit (NeoBioscience, catalog No: EMC001b.96, China), following the instructions provided by the manufacturer. The samples were measured at a wavelength of 450 nm using an enzyme labeling instrument (Multiskan SkyHigh, Thermo Fisher Scientific, Massachusetts, USA).

Quantitative Real-Time Polymerase Chain Reaction (qRT-PCR) Analysis

Total RNA was isolated from colon tissues and cardiac tissues utilizing TRIzol reagent (Thermo Fisher Scientific, Massachusetts, USA). The extracted RNA's concentration and purity were assessed using a NanoDrop ND-1000 spectrophotometer (Thermo Fisher Scientific, USA). After the quantification, cDNA was synthesized using a high-capacity cDNA reverse transcription kit (Thermo Fisher Scientific, Massachusetts, USA). The synthesized cDNA was then prepared for qRT-PCR by dilution and application of PowerUp™ SYBR™ Green Master Mix (Thermo Fisher Scientific, Massachusetts, USA), following the protocol provided by the manufacturer. The qRT-PCR procedure was set as follows: initial incubation at 50°C for 2 minutes, denaturation at 95°C for 2 minutes, followed by 40 cycles of

denaturation at 95°C for 15 seconds and annealing/extension at 60°C for 1 minute. Relative quantification was done by the $2^{-\Delta\Delta Ct}$ method. The specific primer sequences utilized in this analysis are provided in Table 1.

Western Blot Analysis

RIPA lysis buffer (Medical Discovery Leader, Beijing, China) extracted total proteins from intestinal tissues and cardiac tissues. The protein concentrations in the samples were quantified using a BCA protein assay kit (Medical Discovery Leader, Beijing, China). The protein extracts were then subjected to separation via 12% sodium dodecyl sulfate-polyacrylamide gel electrophoresis (SDS-PAGE) and subsequently transferred onto polyvinylidene difluoride (PVDF) membranes. The membranes were incubated in a blocking buffer containing 5% skim milk in Tween 20 (TBST) tri-buffered saline for 2 hours. Following blocking, the membranes were incubated overnight at 4°C with primary antibodies targeted against Occludin (Abcam, 1:1000, ab216327), ZO-1 (Abcam, 1:1000, ab307799), NF-κB p65 (Abcam, 1:1000, ab16502) and β-actin (Abcam, 1:1000, ab8226) as a loading control. The membranes were then exposed to appropriate secondary antibodies for 2 hours at 37°C. Protein bands were detected using an enhanced chemiluminescence (ECL) kit and visualized with a gel documentation system (Bio-Rad, Hercules, CA, USA). The results were analyzed using Image J software, allowing for quantification and comparison of protein expression levels.

Fecal Microbiota Analysis

After administering the final dose, fresh fecal samples were collected from each experimental group under aseptic conditions and immediately placed into lyophilization tubes. These samples were then snap-frozen in liquid nitrogen and stored at −80°C for subsequent analysis. Genomic DNA was extracted from these samples using the PF Mag-Bind Stool DNA Kit (Omega Bio-tek, Georgia, USA), adhering to the instructions provided by the manufacturer. For the analysis of the bacterial community structure, the hypervariable V3-V4 regions of the bacterial 16S rRNA gene were amplified using

Table 1 Primer Sequences of the Target Gene Used in the qRT-PCR Experiment

Genes	Primer sequence (5′ to 3′)
Occludin	Forward: TGAAAGTCCACCTCCTTACAGA
	Reverse: CCGGATAAAAAGAGTACGCTGG
Zo-1	Forward: GCCGCTAAGAGCACAGCAA
	Reverse: GCCCTCCTTTTAACACATCAGA
GAPDH	Forward: TCATCACTATTGGCAACGAGCG
	Reverse: CGGATGTCAACGTCACACTTCA
Cpt1a	Forward: GGGCTTTCACTGTAAGTGTTCAA
	Reverse: TGGTATTTACATGCAATGGACAG
Cpt2	Forward: CTGACCAAAGAAGCAGCGATG
	Reverse: AGAGTGCTGGTGGACAGGATG
CACT	Forward: TGTCTAAATCCCCAGGAGAAAGT
	Reverse: GGGAAAGAATGTGCAAAAGGA
Il-18	Forward: GTGAACCCCAGACCAGACTG
	Reverse: CCTGGAACACGTTTCTGAAAGA
Il-1β	Forward: AAATGCCACCTTTTGACAGTGATG
	Reverse: GCTCTTGTTGATGTGCTGCTG
Caspase-1	Forward: AATACAACCACTCGTACACGTC
	Reverse: AGCTCCAACCCTCGGAGAAA
Gsdmd	Forward: CCATCGGCCTTTGAGAAAGTG
	Reverse: ACACATGAATAACGGGGTTTCC
Nlrp3	Forward: ATTACCCGCCCGAGAAAGG
	Reverse: TCGCAGCAAAGATCCACACAG
β-actin	Forward: GTGACGTTGACATCCGTAAAGA
	Reverse: GTAACAGTCCGCCTAGAAGCAC

https://doi.org/10.2147/DDDT.S504884

the primer pairs 338F (5′-ACTCCTACGGGAGGCAGCAG-3′) and 806R (5′-GGACTACHVGGGTWTCTAAT-3′). This amplification was performed in an ABI GeneAmp® 9700 PCR thermocycler (ABI, CA, USA). The resulting amplicons were then purified and subjected to paired-end sequencing on an Illumina platform, either PE300 or PE250 (Illumina, San Diego, USA), following the standard sequencing protocols established by Majorbio Bio-Pharm Technology Co. Ltd. (Shanghai, China).

Untargeted Metabolomics Analysis

To extract metabolites from blood serum samples, 100 μL of serum was combined with 400 μL of a solution (acetonitrile: methanol = 1:1 (v:v) containing 0.02 mg/mL of the internal standard, L-2-chlorophenylalanine, in a 1.5 mL centrifuge tube. The mixture was vortexed for 30 seconds and then subjected to low-temperature sonication for 30 minutes at 5°C and 40 KHz. The samples were then chilled at −20°C for 30 minutes to facilitate protein precipitation. The samples were centrifuged at 13,000 g and 4°C for 15 minutes. The supernatant was carefully transferred to a new tube and dried under a stream of nitrogen. The dried sample was reconstituted in 100 μL of acetonitrile: water (1:1) solution and again subjected to low-temperature ultrasonication for 5 minutes at 5°C and 40 KHz, followed by centrifugation under the same conditions to pellet any remaining particulates. The clear supernatant was transferred into sample vials for subsequent LC-MS/MS analysis. For quality control, a pooled QC sample was prepared by mixing aliquots from all the samples to monitor the LC-MS/MS system's performance and ensure consistent, reliable results across all analyses.

LC-MS/MS analysis was performed using a Thermo UHPLC-Q Exactive HF-X system with an ACQUITY HSS T3 column. The study utilized two mobile phases: 0.1% formic acid in water and acetonitrile (95:5, v/v) for solvent A and 0.1% formic acid in a mixture of acetonitrile, isopropanol, and water (47.5:47.5:5, v/v) for solvent B, with a flow rate of 0.40 mL/min and a column temperature of 40°C. The mass spectrometer operated in positive and negative ionization modes across a mass range of 70–1050 m/z, with a spray voltage of 3500V and normalized collision energies of 20, 40, and 60eV. The data were acquired in Data Dependent Acquisition (DDA) mode, allowing for high-resolution full MS and MS/MS scans.

The raw LC/MS data were processed using Progenesis QI software for feature detection, alignment, and quantitation. Metabolites were identified by searching against databases like HMDB, Metlin, and the Majorbio Database. Statistical analyses, including principal component analysis (PCA) and orthogonal partial least squares, discriminate analysis (OPLS-DA), was conducted using the ropls R package. Metabolites significantly differentiating the groups were identified based on a variable importance in projection (VIP) value greater than 1 and a p-value less than 0.05, highlighting fundamental metabolic changes between the compared groups.

Network Pharmacology Analysis

The keyword "allicin" was utilized to search for potential therapeutic target genes in the SwissTargetPrediction (http://www.swisstargetprediction.ch/), STITCH (http://stitch.embl.de/), TCM-Suite (http://TCM-Suite.AImicrobiome.cn), TM-MC (https://tm-mc.kr/), HERB (http://herb.ac.cn/) databases, as well as published literature. Utilizing "myocardial infarction" and "acute myocardial infarction" as the key terms, the "Homo sapiens" species were selected for the extraction of AMI-related target genes using the GeneCards (https://www.genecards.org/), DisGeNet (http://www.disgenet.org/home/) and Online Mendelian Inheritance in Man database (OMIM, https://omim.org/) databases. To identify the intersection target genes of allicin in AMI treatment, R v4.0.1 (https://www.r-project.org/) was used to find the overlapping disease and drug targets and create a Venn diagram. Then, the STRING database (https://string-db.org/) was used to perform protein-protein interaction (PPI) research on potential genes and proteins. GO enrichment analysis and KEGG pathway annotation were performed using R v4.0.1.

Statistical Analysis

Statistical evaluations were conducted utilizing SPSS 26 (SPSS Inc., Chicago, IL, USA) and GraphPad Prism 8 (GraphPad Software, San Diego, CA, USA). Variables conforming to parametric distribution criteria were expressed as the mean ± standard deviation (SD) and subjected to intergroup comparisons through One-way analysis of variance

(One-way ANOVA). Conversely, non-parametric variables were delineated as medians accompanied by interquartile ranges, with comparative analysis performed via Wilcoxon rank-sum tests. A p-value of less than 0.05 was designated as the threshold for statistical significance.

Results

Allicin Administration Protected Cardiac Function After AMI and Improved Myocardial Tissue Damage

The protocol for drug administration is depicted in Figure 1A. To elucidate the effects of allicin on myocardial tissue post-AMI, we employed histological staining techniques, including Hematoxylin and Eosin (HE) and Masson's trichrome staining, to assess myocardial samples. HE staining highlighted that cardiomyocytes in the sham group were well-organized and compactly arranged, whereas those in the model group appeared disorganized, with cells exhibiting pyknotic nuclei and significant infiltration by inflammatory cells, as shown in Figure 1B. Allicin treatment mitigated these pathological alterations when compared to the model group. Furthermore, Masson's trichrome staining, illustrated in Figure 1C, demonstrated extensive necrosis and replacement by collagen fibers in the model group's myocardial tissue, especially within the left ventricular wall, in contrast to the sham group. Allicin administration notably reduced collagen deposition and ameliorated myocardial fibrosis, suggesting a decrease in myocardial infarction size.

Echocardiographic evaluations, presented in Figure 1D and E, corroborated the structural observations with functional outcomes, revealing a significant decrease in LVEF and LVFS ($P < 0.01$), alongside an increase in LVIDd and LVIDs ($P < 0.01$) in the model group as opposed to the sham group. This confirmed the effective induction of AMI in the mouse model. Remarkably, oral administration of allicin for 28 days led to a significant improvement in LVEF and LVFS ($P < 0.01$) and a reduction in LVIDd and LVIDs ($P < 0.01$), indicating enhanced myocardial contraction functions.[19] In summary, these findings collectively suggest that allicin has a therapeutic potential in ameliorating myocardial fibrosis, reducing infarct size, and improving overall cardiac function following AMI.

Allicin Treatment Mitigated AMI-Induced Disruptions in Intestinal Barrier Function

To elucidate the effects of allicin on intestinal barrier function, we investigated the morphological alterations in intestinal tissues of mice using Hematoxylin and Eosin (H&E) staining, as illustrated in Figure 2A. Colonic sections from the sham group displayed intact epithelial layers, well-organized crypt structures, and uniformly distributed goblet cells. In contrast, the model group exhibited significant colonic damage, characterized by substantial infiltration by inflammatory cells and disarrayed structure of crypts and goblet cells. Notably, allicin intervention ameliorated these pathological manifestations to a considerable extent. Furthermore, we evaluated the expression of ZO-1 and Occludin in the colon, key biomarkers of intestinal barrier integrity, to determine the impact of allicin on the intestinal barrier in AMI mice. Figure 2E and F shown that mRNA levels of Occludin and ZO-1 were decreased in the model group compared to the sham group ($P < 0.05$). However, allicin treatment significantly restored their transcription levels of ZO-1 and Occludin ($P < 0.01$).

To corroborate these findings, we also assessed the protein expression levels of ZO-1 and Occludin through Western Blot analysis, as depicted in Figure 2B–D. The model group showed significantly lower expression levels of ZO-1 and Occludin relative to the sham group ($P < 0.01$), indicating compromised intestinal barrier function following AMI. Allicin administration markedly increased the expression of these proteins ($P < 0.05$), suggesting that allicin effectively contributed to the partial restoration of the intestinal barrier in AMI mice. These results indicate that allicin treatment mitigates AMI-induced disruptions in intestinal barrier function.

Allicin Remodeled the Gut Microbiota Disorder After AMI

The onset of AMI is frequently accompanied by alterations in gut microbiota composition and function. To assess the potential impact of allicin on the intestinal flora, we analyzed the fecal microbiota of AMI mice through macrogenomic sequencing. In the α-diversity analysis, the Shannon index, measuring species diversity, and the Chao1 index, assessing community richness, were utilized. Results depicted in Figure 3A illustrate a significant reduction in community richness

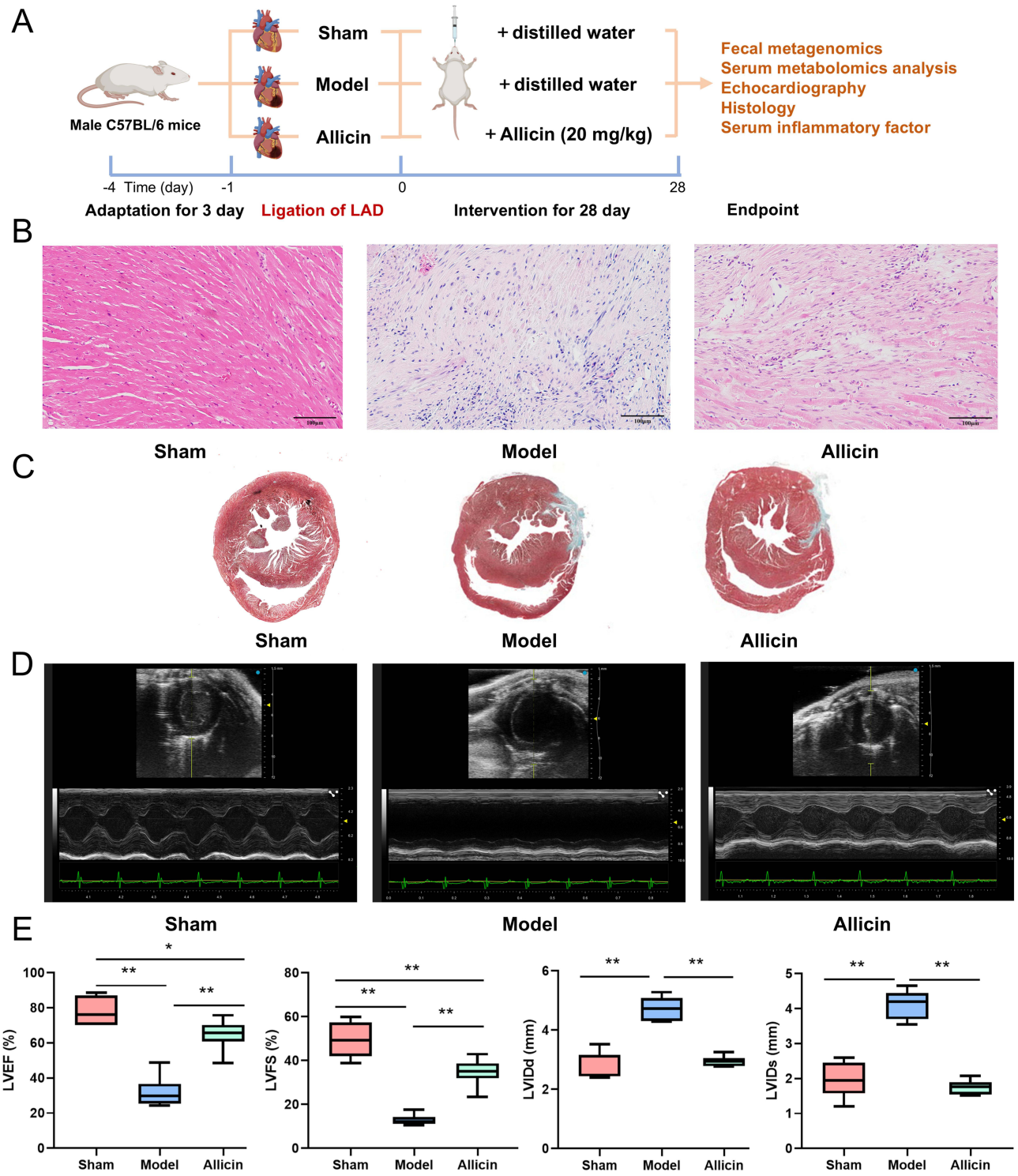

Figure 1 Allicin's Cardioprotective Effects Post-AMI. (**A**) Schematic representation of allicin administration in mice following AMI. (**B**) Heart sections stained with Hematoxylin and Eosin (H&E), illustrating histological features (scale bar: 100 μm). (**C**) Heart sections subjected to Masson's trichrome staining. (**D**) Echocardiographic images showcasing the left ventricular function. (**E**) Quantitative analysis of left ventricular ejection fraction (LVEF), fractional shortening (LVFS), left ventricular internal end-diastolic (LVIDd), and end-systolic (LVIDs) diameters; n=6. Data are presented as mean ± standard deviation. Significance levels are denoted as *$P < 0.05$, and **$P < 0.01$.

in AMI mice compared to the sham group, a trend reversed upon allicin treatment ($P < 0.05$). Moreover, AMI induced a notable increase in species diversity, as evidenced by higher Shannon indexes ($P < 0.05$) shown in Figure 3B. Allicin appeared to normalize this disturbed diversity, although not significantly ($P > 0.05$), suggesting a simplification and homogenization of the gut microbial community post-AMI with allicin treatment. Principal coordinate analysis (PCoA)

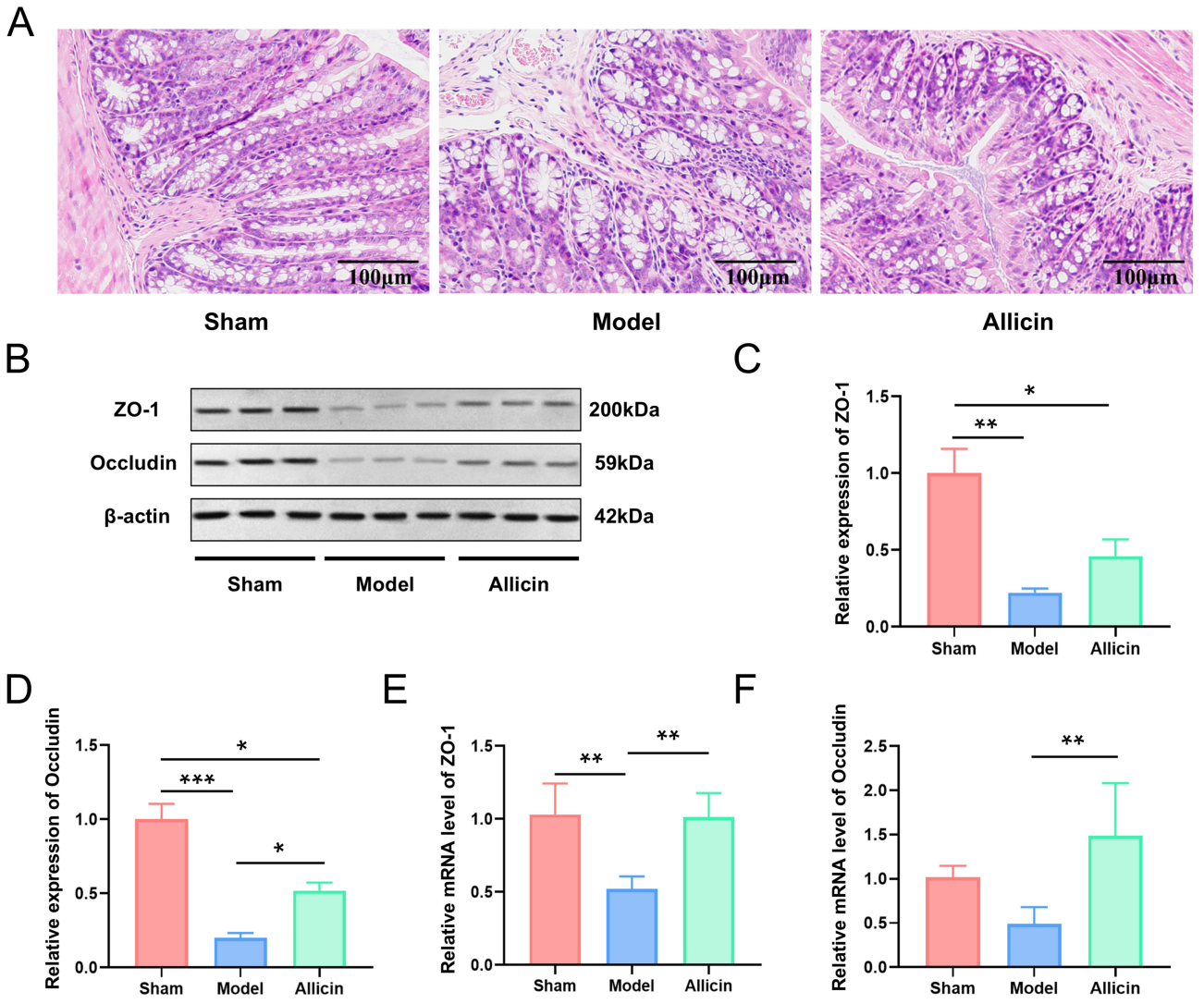

Figure 2 Allicin Enhances Intestinal Barrier Integrity after AMI. (**A**) Histopathological assessment of colon tissues via H&E staining (scale bar: 100 μm). (**B**–**D**) Western blot analysis of colonic ZO-1, Occludin, and β-actin protein expression; n=3. (**E** and **F**) Quantitative real-time PCR (qRT-PCR) evaluation of colonic ZO-1 and Occludin mRNA levels across different groups; n=6. Results are expressed as mean ± standard deviation. Significance indicated by *$P < 0.01$, **$P < 0.001$, and ***$P < 0.0001$.

further demonstrated distinct separations among the three groups, highlighting significant beta diversity differences (Figure 3C). ANOSIM analysis confirmed these observations (R = 0.611, P = 0.001, Figure 3D), indicating that AMI markedly altered the gut microbiota. At the same time, the allicin administration reshaped it towards the sham group profile.

Further investigation into the overall structure of gut microbial species revealed AMI-induced shifts in the relative abundance at different taxonomic levels. The dominant phyla across all groups were *g_Bacteroidetes* and *g_Firmicutes* (Figure 3E). AMI was associated with an increased relative abundance of *g_Firmicutes* and a decreased abundance of *g_Bacteroidetes* compared to the sham group, resulting in a higher *g_Firmicutes* to *g_Bacteroidetes* ratio, indicative of dysbiosis (Figure 3F–H). Allicin intervention modulated these changes, suggesting a restorative effect on the intestinal flora imbalance (Figure 3H). At the genus level, significant alterations in bacterial abundance were noted (Figure 3I). Linear discriminant analysis and Effect Size (LEfSe) identified specific bacterial genera that were differentially enriched across groups. Notably, genera such as *g_unclassified_f_Erysipelotrichaceae, g_unclassified_p_Firmicutes*, and *g_Parasutterella* were predominant in the model group, while *g_Lactobacillus, g_Prevotella, g_Alistipes, g_Limosilactobacillus, g_Helicobacter*, and *g_Odoribacter* were significantly enriched in the allicin-treated groups

https://doi.org/10.2147/DDDT.S504884

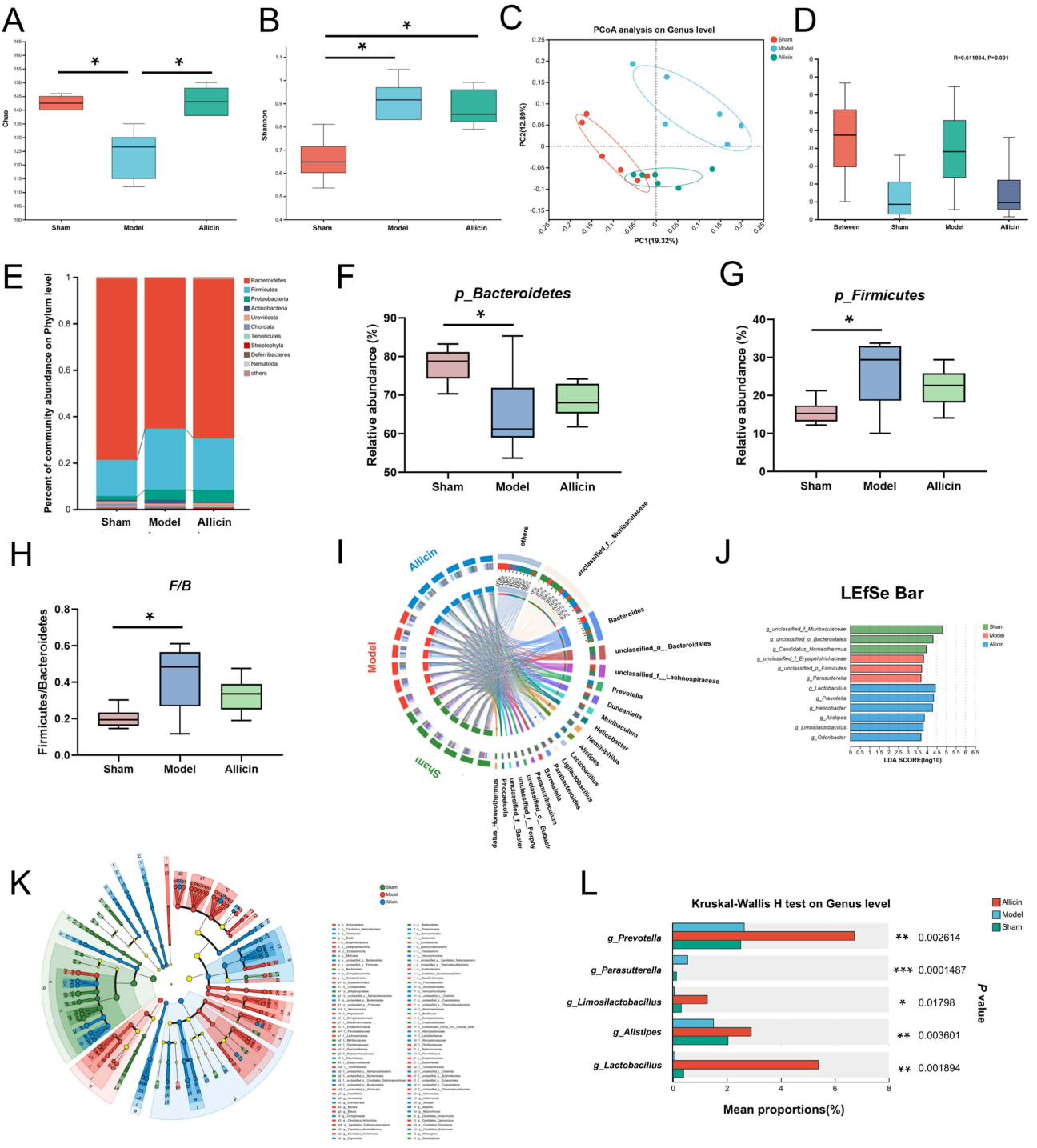

Figure 3 Allicin Mitigates AMI-Induced Intestinal Dysbiosis. (**A** and **B**) Evaluation of alpha diversity in the intestinal microbiota of sham, model, and allicin-treated groups using Chao1 and Shannon indices. (**C**) Principal coordinates analysis (PCoA) of genus-level intestinal microbiome composition based on Bray-Curtis distances. (**D**) Analysis of similarities (ANOSIM) assessing microbial community structure differences between groups. (**E**) Phylum-level relative abundances of intestinal bacteria in sham, model, and allicin groups. Comparative analyses of relative abundances of (**F**) Firmicutes and (**G**) Bacteroidetes, and (**H**) the Firmicutes to Bacteroidetes ratio. (**I**) Circos plot depicting the ten most abundant bacterial genera. (**J**) Linear discriminant analysis effect size (LEfSe) identifying key genus-level biomarkers. Only taxa with a significant LDA score (>3.5) are shown. (**K**) Cladogram illustrating differential microbiota from species to genus levels. (**L**) Genus-level fecal microbiota comparisons across groups were analyzed using the Wilcoxon rank-sum test and presented as medians with interquartile ranges. n=6, with significance marked as *$P < 0.05$, **$P < 0.01$, and ***$P < 0.001$.

(Figure 3J and K). The Kruskal–Wallis *H*-test revealed that AMI increased the abundance of *g_Parasutterella* and decreased that of beneficial genera, including *g_Lactobacillus, g_Prevotella, g_Alistipes*, and *g_Limosilactobacillus*, which was significantly counteracted by allicin treatment (Figure 3L). These findings suggest that allicin effectively

 https://doi.org/10.2147/DDDT.S504884

ameliorates the deleterious alterations in gut microbiota structure induced by AMI, potentially conferring beneficial effects on the host's health.

Allicin Enhanced Myocardial Energy Metabolism Flexibility Through Modulating Metabolites and Key Enzymes Associated with the Fatty Acid Metabolic Pathway

To assess the impact of allicin on the alterations in gut metabolites following AMI, an untargeted metabolomics approach was employed using UHPLC-QE-MS on serum samples. Partial least squares discriminant analysis (PLS-DA) models demonstrated distinct clustering within groups and clear separation between the groups (Figure 4A and B), with the metabolic profile of the allicin group closely resembling that of the sham group. The reliability of the PLS-DA model was further validated through a 200-times-permutation test, which confirmed the model's accuracy and indicated no overfitting, as evidenced by lower R^2 and Q^2 values from the permutation than those from the original model and a negative intercept of the blue Q^2 regression line (Figure 4C and D).

Differential metabolic products associated with allicin treatment were identified using orthogonal projections to latent structures discriminant analysis (OPLS-DA), taking into account both the variable importance in projection (VIP > 1) and p-values ($P < 0.05$) from *t*-tests (Tables S1 and S2). This analysis revealed significant differences in metabolite profiles between groups, with 61 differential metabolites detected in positive ion mode and 52 in negative ion mode between the model and sham groups (Figure 4E). Comparatively, 86 differential metabolites in positive mode and 81 in negative mode were identified between the allicin and model groups (Figure 4F).

It is worth noting that in the comparison of three groups of differential metabolites, a total of 29 differential metabolites were found to recover to normal levels to varying degrees after allicin administration, including L-Carnitine, L-Palmitoylcarnitine, Deoxyuridine, PE (16:0/0:0), and so on. This indicates that allicin has a significant improvement effect on metabolic disorders after AMI (Table S3). These small molecule metabolites, believed to be regulated by allicin's efficacy, mainly originate from amino acid, glycerophospholipids, fatty acids, nucleotides and other categories. Cluster heatmap analysis was performed on the top 10 selected differential metabolites, revealing that the sham and allicin groups clustered together and showed distinct differences from the model group (Figure 4G). Analysis of common differential metabolites highlighted their enrichment in key metabolic pathways such as fatty acid metabolism, linoleic acid metabolism, glycine, serine and threonine metabolism and bile secretion, emphasizing the comprehensive impact of allicin on AMI-interfering metabolic pathways (Figure 4H).

Research has found that the remodelling of fatty acid metabolism is considered one of the key driving factors in the development of HF after AMI.[20] The abnormal changes in myocardial fatty acid metabolism after AMI are related to the transcriptional changes of multiple key enzymes involved in its metabolic pathway.[21] The significant enrichment of fatty acid metabolic pathways suggests that the therapeutic benefits of allicin may be closely related to improving energy metabolism disorders after myocardial infarction. Therefore, we further examined the gene expression levels of key enzymes involved in cardiac tissue's fatty acid beta-oxidation pathway. Compared to the sham-operated group, there was a significant decrease in gene expression of CPT1a, CPT2, and CACT enzymes in cardiac tissue from the model group ($P < 0.001$), indicating impaired fatty acid beta-oxidation and abnormal cardiac energy metabolism (Figure 4I). However, allicin treatment significantly enhanced the expression of CPT1a, CPT2, and CACT enzymes promoting fatty acid beta-oxidation and improving flexibility in cardiac energy metabolism ($P < 0.01$). These results indicated that the allicin could regulate the expression of multiple key enzymes to affect fatty acid metabolism and improve the prognosis of AMI.

Network Pharmacology Predicted Potential Allicin Mechanisms in AMI Treatment

We used network pharmacology to understand better the molecular mechanisms of allicin in treating AMI. Using Network Pharmacology analysis, allicin and shared 122 putative targets with the acquired 5370 AMI-relevant genes (Figure 5A). Based on these shared genes, a final PPI network with 41 hub genes was established with the median values (BC > 43.09, CC > 0.47, DC > 14, EC > 0.048, LAC > 6.4, NC > 8.99), including IL-18, IL-1β, NF-κB p65, NLRP3, caspase-1 (Figure 5B). GO and KEGG analysis demonstrated that these shared genes were enriched in signaling pathways associated with inflammatory responses and death receptor signaling, including pyroptosis, the NLRP3

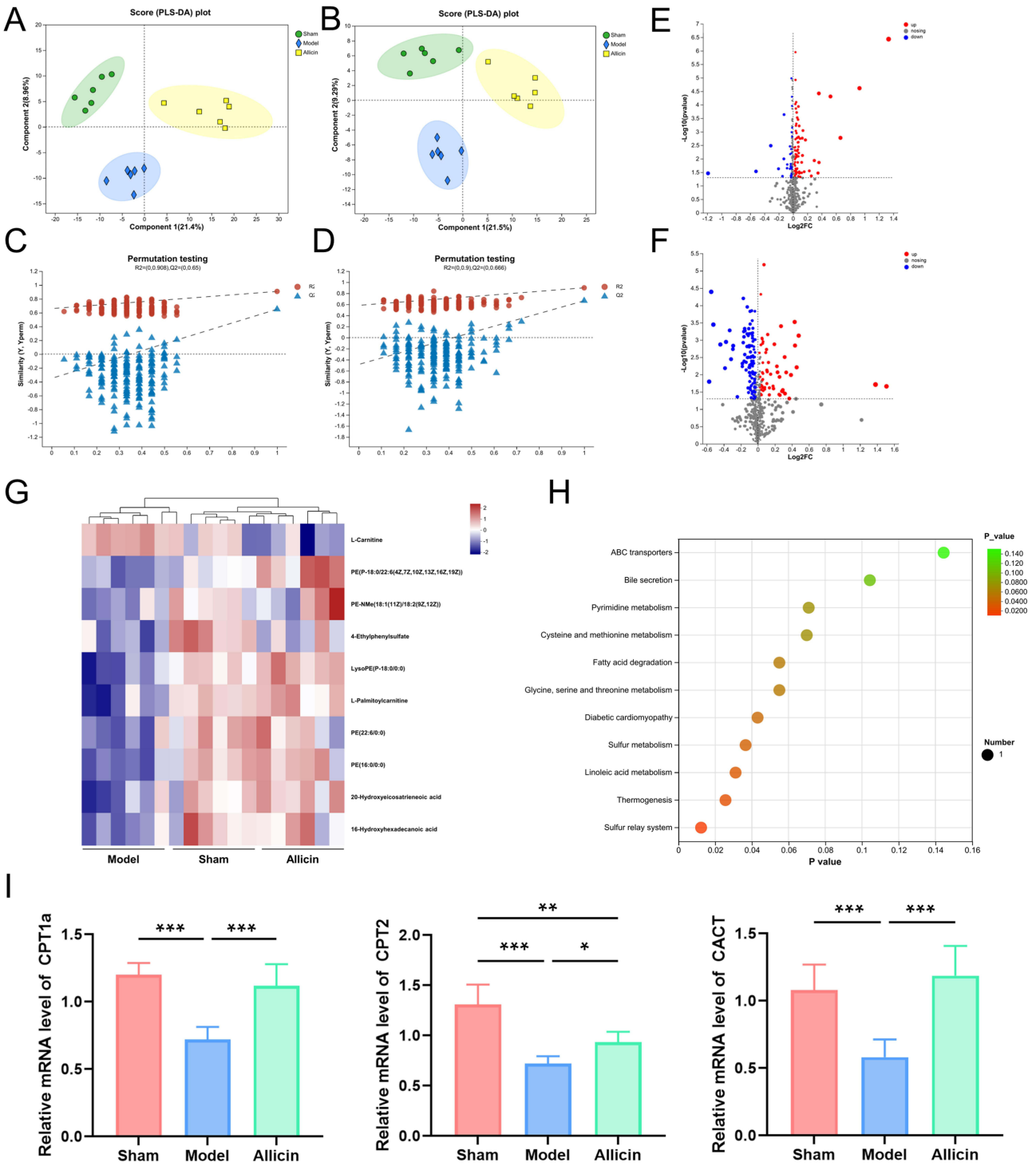

Figure 4 Impact of Allicin on the Serum Metabolic Profile in AMI Mice. Partial least squares discriminant analysis (PLS-DA) score plots depicting variations in metabolites under (**A**) positive and (**B**) negative ion modes illustrate the metabolic alterations induced by allicin. (**C**) The reliability of the PLS-DA model was validated through a 200-times-permutation test between model and sham groups. (**D**) The reliability of the PLS-DA model was validated through a 200-times-permutation test between allicin and model groups. (**E**) Volcano plot highlighting differentially accumulated metabolites between model and sham groups. (**F**) Volcano plot elucidating the differentially accumulated metabolites between allicin-treated and model groups. (**G**) A heatmap presents the top 10 differential metabolites across the three groups, offering insights into the metabolic impact of allicin treatment. (**H**) Kyoto Encyclopedia of Genes and Genomes (KEGG) pathway enrichment analysis based on altered metabolites reveals the metabolic pathways influenced by allicin. (**I**) qRT-PCR evaluation of cardiac CPT1a, CACT and CPT2 mRNA levels across different groups; n=6. Statistical significance is denoted as *$P < 0.05$, **$P < 0.001$, and ***$P < 0.0001$.

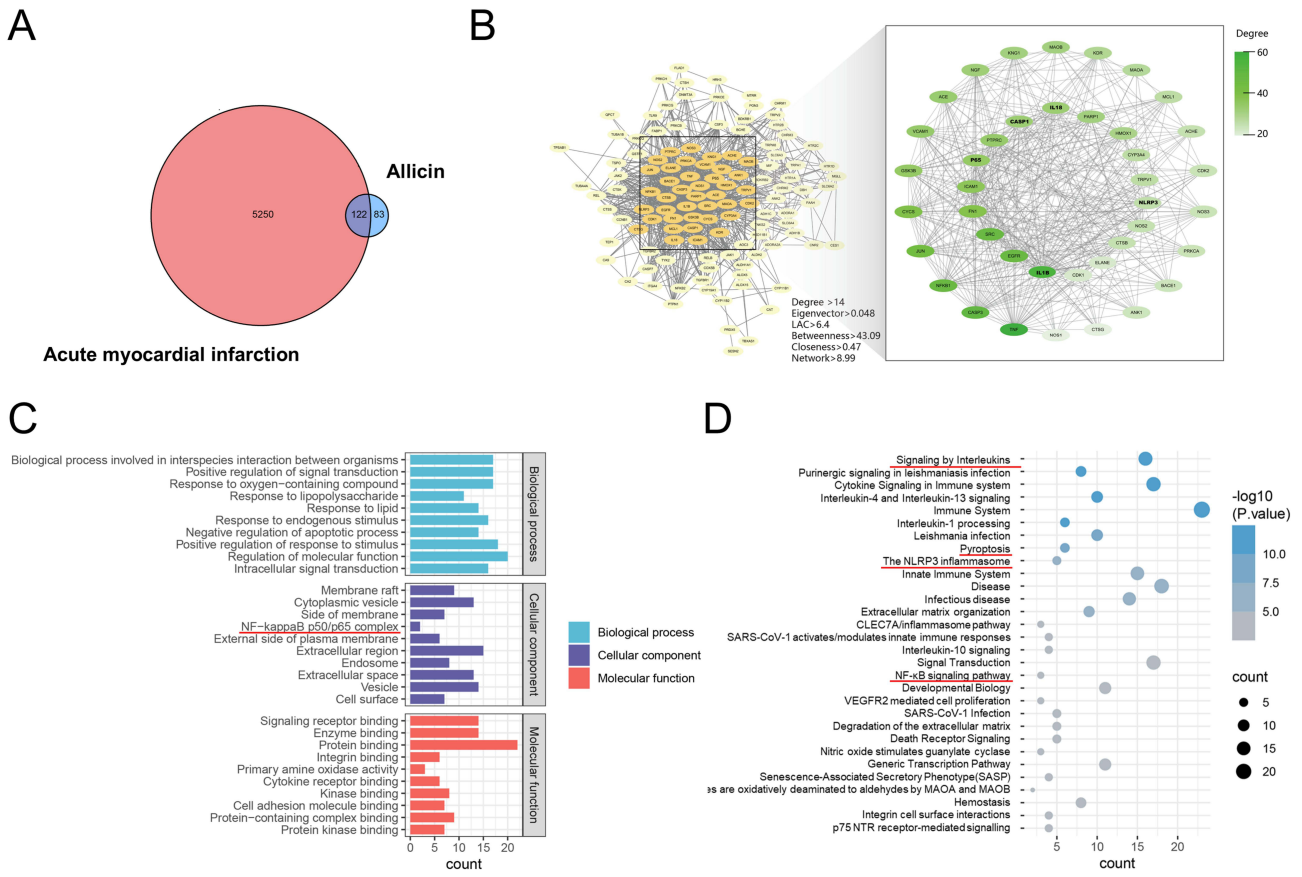

Figure 5 Network Pharmacology Prediction for Allicin Treatment of AMI. (**A**) Venn plot illustrates the shared targets between allicin and AMI. (**B**) PPI network shows the identification of allicin's core candidate targets against AMI. (**C**) GO enrichment analysis of the potential targets of allicin for improving AMI in three terms: (BP), molecular function (MF), and cellular component (CC). (**D**) KEGG pathway analysis of the potential targets of allicin in improving AMI.

inflammasome, NF-κB signaling pathway, apoptosis and multiple interleukins signaling. (Figure 5C and D). Therefore, the primary mechanism of allicin in improving AMI might be related to the NF-κB signaling pathway, NLRP3/Caspase-1 pathway, and other pathways.

Allicin Inhibited NF-κB-Mediated NLRP3/Caspase-1/GSDMD Pathway to Suppress Pyroptosis and Reduce Inflammatory Response After AMI

Given the integrated analyses of network pharmacology, metagenomic, and metabolomic results, we hypothesized that NF-κB/NLRP3/caspase-1 mediated pyroptosis was a critical mechanism of allicin in improving inflammatory response after AMI. Therefore, we assessed the influences of allicin on the NF-κB/NLRP3/caspase-1 signaling pathway in the cardiac tissue by Western blot and qRT-PCR. NF-κB p65 expression in the AMI mice model showed significant overexpression compared to controls ($P < 0.5$), demonstrating activation of the inflammatory response (Figure 6A and B). Compared with the model group, allicin treatment could reverse this trend ($P < 0.5$). In Figure 6C–G, qRT-PCR results showed that the mRNA expressions of NLRP3, Caspase-1, GSDMD, IL-18, and IL-1β were increased in the model group ($P < 0.5$). This response was reversed by allicin treatment ($P < 0.5$). We demonstrated the remarkable changes in the signaling pathway components, suggesting that the NF-κB/NLRP3/caspase-1 signaling pathway was activated by AMI, which allicin could reverse.

Furthermore, the involvement of multiple inflammatory mediators in the onset and progression of AMI is well-documented. IL-18 and IL-1β, recognized as vital pro-inflammatory cytokines, play crucial roles in modulating the balance between anti-inflammatory and pro-inflammatory responses following AMI.[22] Furthermore, evidence suggests their contributory role in exacerbating intestinal barrier dysfunction and mucosal injury.[23] Given their detrimental impact

https://doi.org/10.2147/DDDT.S504884

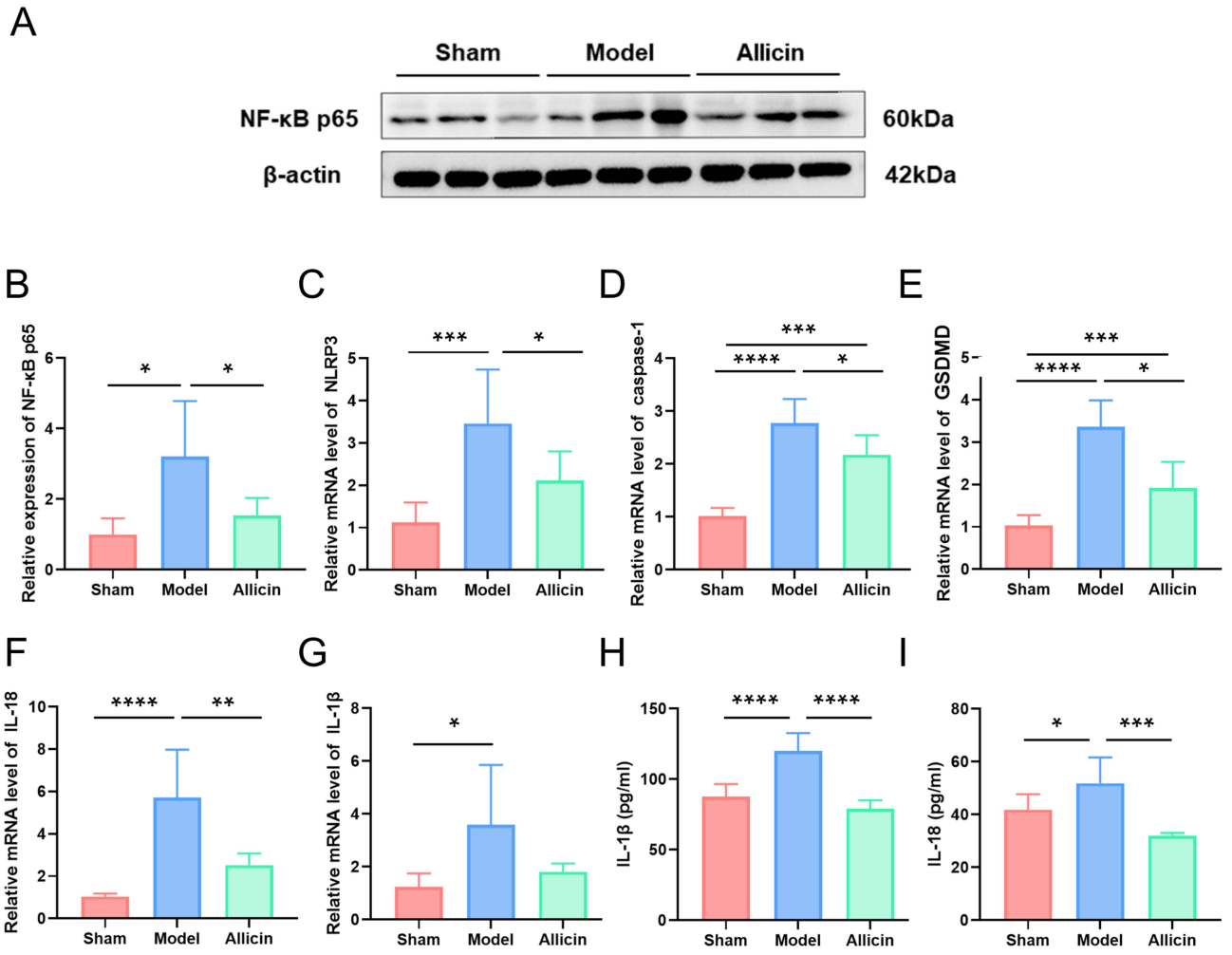

Figure 6 Allicin Inhibited NF-κB-mediated NLRP3/Caspase-1/GSDMD Pathway to Suppress Pyroptosis and Reduce Inflammatory Response after AMI. (**A** and **B**) Western blot analysis of NF-κB and β-actin protein expression; n=3. (**C**–**G**) qRT-PCR evaluation of cardiac NLRP3, Caspase-1, GSDMD, IL-18 and IL-1β mRNA levels across different groups; n=6. (**H** and **I**) Serum levels of IL-1β and IL-18 measured by enzyme-linked immunosorbent assay (ELISA); n=6. Results are expressed as mean ± standard deviation. Significance indicated by *$P < 0.05$, **$P < 0.01$, ***$P < 0.001$ and ****$P < 0.0001$.

on intestinal integrity, we assessed the serum levels of these inflammatory cytokines (Figure 6H and I). Our findings revealed a significant elevation in the levels of IL-18 and IL-1β in the model group compared to the sham group, indicating a pronounced inflammatory response triggered by AMI. Conversely, allicin treatment substantially mitigated the increased levels of these cytokines, displaying a pronounced anti-inflammatory effect. These observations collectively suggest that allicin may alleviate inflammatory damage, thereby offering protective benefits to cardiac function and intestinal barrier integrity post-AMI.

Correlations of Gut Microbiota, Serum Metabolites, and Host Phenotypes

Spearman correlation analysis was conducted to explore the intricate relationships among gut microbiota, serum metabolite levels, and host phenotype. This analysis unveiled significant correlations between serum metabolites and key cardiac function metrics. Specifically, phosphatidylethanolamines (PE) (16:0/0:0), PE-NMe (18:1(11Z)118:2 (9Z,12Z)), L-Palmitoylcarnitine, LySoPE (P-18:0/0:0), and 4-Ethylphenylsulfate were found to be positively correlated with LVEF and LVFS, and negatively correlated with LVIDs and LVIDd (Figure 7A). L-carnitine exhibited a noteworthy positive correlation with pro-inflammatory cytokines IL-1β and IL-18 while showing a negative correlation with LVIDs and LVIDd. Other metabolites displayed significant inverse correlations with IL-1β and IL-18 (Figure 7B). Moreover, as illustrated in Figure 7C, a profound relationship exists between the composition of the intestinal flora and inflammatory

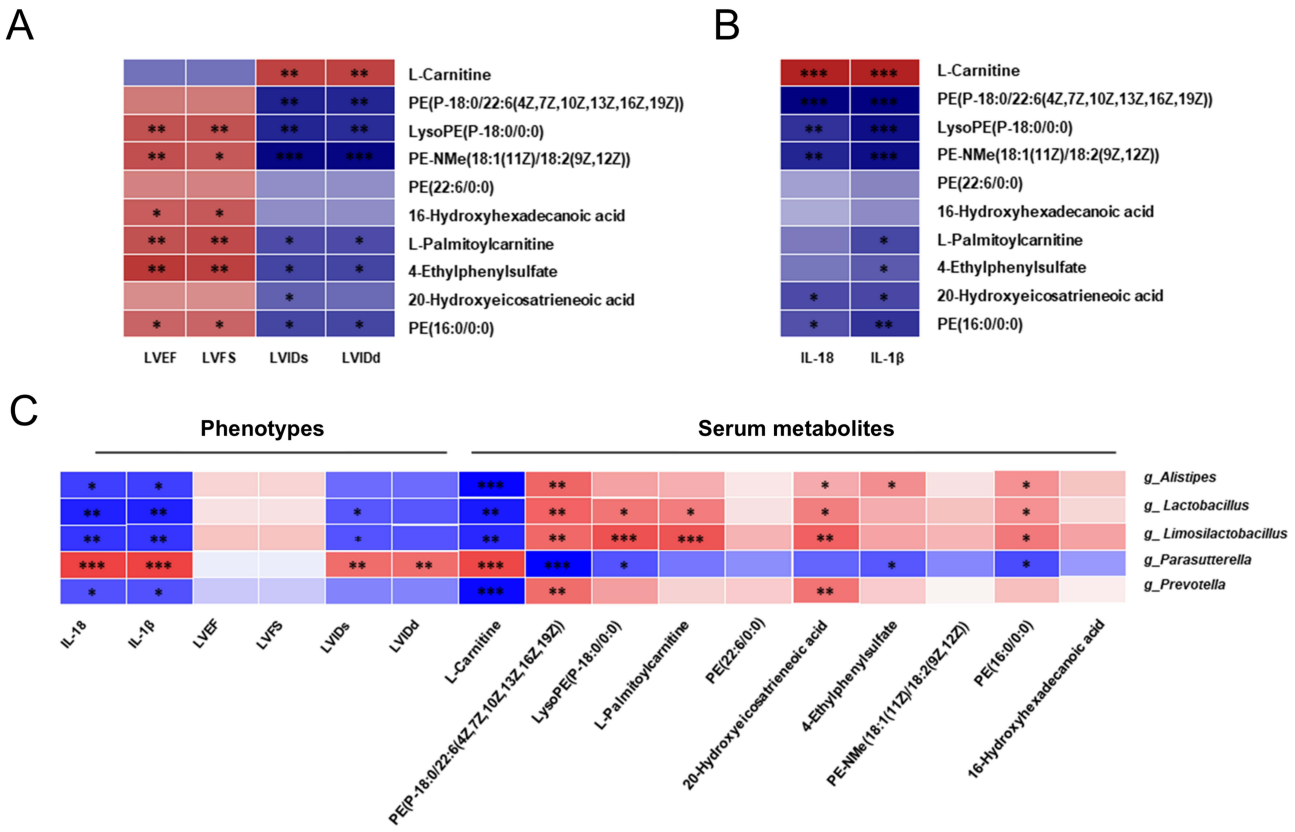

Figure 7 Correlation Analysis of Key Efficacy Indicators with Gut Microbiota and Serum Differential Metabolites. (**A**) Heatmap analysis demonstrating Spearman correlations between cardiac function and signature metabolites. (**B**) Heatmap analysis demonstrating Spearman correlations between inflammatory factors and signature metabolites. (**C**) Heatmap analysis revealing Spearman correlations among gut microbiota composition, key efficacy indicators, and signature metabolites, underscoring the intricate interactions within the gut-heart axis post-AMI. Data are expressed as mean ± standard error of the mean. Inter-group comparisons were performed using Student's *t*-tests; n=6. Significance levels are indicated by *$P < 0.05$, **$P < 0.01$, and ***$P < 0.001$.

markers post-AMI. IL-1β and IL-18 were significantly negatively correlated with beneficial bacteria such as *g_Alistipes, g_Lactobacillus, g_Limosilactobacillus*, and *g_Prevotella* and positively correlated with *g_Parasutterella*. L-carnitine was notably negatively correlated with beneficial bacteria and positively with *g_Parasutterella*, while L-Palmitoylcarnitine was significantly positively correlated with *g_Lactobacillus* and *g_Limosilactobacillus*. These results indicate a complex interplay between gut microbiota, serum metabolites, and host health, particularly in the aftermath of AMI.

Discussion

AMI, a principal cause of heart failure (HF) and cardiac death globally, is influenced by a blend of genetic and environmental factors. Despite advancements in therapeutic interventions such as percutaneous coronary intervention (PCI) and pharmacotherapy, a significant portion of AMI patients, approximately 48%, experience left ventricular (LV) remodeling within the first year post-infarction.[24] This underscores the critical importance of further elucidating the underlying mechanisms of AMI and exploring innovative treatment strategies. Recent studies have illuminated a link between AMI and alterations in the gut microbiota's composition and diversity, suggesting a pivotal role for the gut microbiota in developing therapeutic strategies for AMI.[25]

Diet, as a significant modulator of gut microbiota, indicates that alterations in dietary patterns could be a strategic approach to AMI treatment. Historically used as a condiment and in folk medicine, Garlic is known for its antimicrobial, antiatherosclerotic, antihypertensive, and cardioprotective effects. Allicin, a sulfur-containing compound in Garlic, has been identified as the primary bioactive component contributing to the cardiovascular protective benefits of Garlic.[26] Studies have demonstrated allicin's capacity to modulate the intestinal microbiota, enhance intestinal barrier function,

https://doi.org/10.2147/DDDT.S504884

and protect against bacterial endotoxin-induced damage in various disease models.[27–29] Recent research has shown that allicin can ameliorate aortic lesions by altering the gut microbiome and metabolites in L-carnitine-induced atherosclerotic ApoE$^{-/-}$ mice.[30] However, the therapeutic benefits of allicin in AMI treatment, particularly its effects on the intestinal tract and flora, remain insufficiently explored.

It is noteworthy that AMI is associated with increased intestinal wall permeability due to compromised cardiac output and reduced intestinal perfusion. This breakdown in the gut barrier facilitates the translocation of lipopolysaccharides (LPS) and gut microbes into the systemic circulation, inducing further systemic inflammation and elevating the risk of cardiovascular events post-MI. Consequently, the intestinal barrier represents a critical nexus in the communication between the gut microbiota and the heart post-AMI.[31] Dysfunction of the intestinal barrier is characterized by the impairment of tight junction proteins, including Occludin and ZO-1, essential for maintaining the integrity of the intestinal barrier.[32] Our study found that oral administration of allicin for 28 days significantly improved myocardial fibrosis, reduced myocardial infarct size, and enhanced gut barrier integrity. Increased expressions of ZO-1 and Occludin and restoration of cardiac function accompanied these effects.

The gut microbiota, a complex and dynamic ecosystem, is crucial for maintaining enteric barrier integrity and gut homeostasis. Our investigation into the overall structure of intestinal flora demonstrated that alpha diversity analysis revealed that allicin treatment significantly enhanced gut microbiota richness in AMI mice. Beta diversity analysis suggested allicin could normalize the intestinal flora composition in AMI mice. An altered ratio of phylum Firmicutes to phylum Bacteroidetes, considered an essential indicator of gut microbiota dysbiosis, was observed.[33] Our findings align with prior research, showing an increase in the relative abundance of phylum Firmicutes and a decrease in phylum Bacteroidetes in AMI mice, leading to an elevated F/B value. Allicin treatment mitigated these AMI-induced disparities in gut flora toward normal levels.

Further analysis revealed that allicin treatments significantly corrected the imbalance between beneficial and harmful bacteria at the genus level of AMI, characterized by increased relative abundances of *g_Lactobacillus, g_Prevotella, g_Alistipes*, and *g_Limosilactobacillus*, and decreased abundance of *g_Parasutterella*. Notably, *g_Prevotella* had been reported to decrease significantly in young men with ST-elevation myocardial infarction (STEMI), negatively correlated with body mass index (BMI) and systolic blood pressure (SBP).[34] *g_Alistipes* was found to be negatively correlated with BNP levels in patients with chronic heart failure.[35] These results suggest that the decrease of these beneficial bacterial genera may predict the poor prognosis of AMI. The *g_Limosilactobacillus* had been considered a beneficial bacterial genus to promote host health benefits, including the modulation of gut microbiota, improvement of metabolic parameters, and antihypertensive, antioxidant, and anti-inflammatory effects.[36,37] Allicin treatment significantly increased the abundance of these beneficial bacterial genera in AMI mice.

Moreover, allicin treatment also significantly induced *g_Lactobacillus* abundance in AMI mice, aligning with research suggesting its antimicrobial activity against pathogens and reinforcement of the intestinal barrier could facilitate gut microbial remodeling and alleviate cardiovascular disease symptoms.[38] Studies found that the abundance of *g_Lactobacillus* in patients with acute coronary syndrome (ACS) was significantly reduced, with higher levels associated with a reduced risk of major adverse cardiovascular events (MACE).[39] AMI subjects with elevated genus Lactobacillus levels had a lower risk of MACE,[40] and a lower level in ACS patients, especially in AMI, was independently linked to the risk of coronary lesions, all-cause death, and cardiac death.[41] Therefore, the cardioprotective effects of allicin may be related to increasing the abundance of these beneficial bacteria after AMI. Meanwhile, *g_Parasutterella*, characterized by succinic acid production inducing inflammation through IL-1β production,[42] was enriched in AMI mice in our study. Elevated succinic acid has been closely associated with the progression of heart failure.[43] Allicin treatment can effectively reverse the increase of *g_Parasutterella* in AMI mice. Therefore, our findings above indicate that allicin supplementation post-AMI increased beneficial symbiotic bacterial communities and suppressed harmful ones, suggesting these cardioprotective effects may result from a synergy between increased beneficial strains and reduced harmful strains in the intestinal flora.

The untargeted metabolomics analysis revealed alterations in microbial-dependent metabolic pathways and associated metabolites implicated in the host disease progression. Our findings demonstrated that allicin-mediated regulation of differential metabolites was closely linked to multiple metabolic pathways, with particular emphasis on fatty acid

degradation, glycerophospholipid metabolism, and linoleic acid metabolism. These results suggest that allicin may have potential therapeutic effects on AMI by modulating these key metabolic pathways. Studies confirm that the energy cardiac muscle needs to maintain proper function is supplied by adenosine triphosphate (ATP) production through the breakdown of fatty acids. In the entire process of fatty acid β-oxidation, the entry of long-chain fatty acyl-coenzyme A(CoA) into mitochondria represents a pivotal step restricting the rate of fatty acid β-oxidation. Carnitine palmitoyl transferase 1 (CPT1), an essential enzyme in the outer mitochondrial membrane, facilitates the conjugation of long-chain fatty acyl-CoA with carnitine to form fatty acylcarnitine. This complex is transported across the inner mitochondrial membrane by carnitine/acylcarnitine translocase (CACT). Subsequently, fatty acylcarnitine is catalyzed by CPT2 in the inner mitochondrial membrane and oxidized by the respiratory chain to produce ATP to maintain normal cardiac energy metabolism.[44] Studies have revealed that AMI leads to energy deficiency and metabolic disorders in the heart, potentially due to impaired mitochondrial fatty acid oxidation in the myocardium, resulting in myocardial cell death and exacerbating the poor prognosis of AMI.[45] Our study observed a significant decrease in the expression levels of key enzymes involved in fatty acid β-oxidation, namely CPT1a, CACT, and CPT2, within the myocardial tissue after AMI.

Additionally, multiple differential metabolites related to the fatty acid oxidation pathway exhibited abnormal expression levels post-AMI, including L-carnitine, L-Palmitoylcarnitine, etc. These findings suggest an aberrant state of myocardial energy metabolism following AMI. L-carnitine assists in transporting fatty acid molecules to the mitochondria for oxidative decomposition under the action of key fatty acid oxidase, thereby releasing energy.[46] Our research results show that allicin increased the expression levels of CPT1a, CACT, and CPT2 genes in cardiac tissue, enhanced the transport of L-carnitine into the mitochondria and fatty acid beta-oxidation, and thus reduced the serum level of L-carnitine. Studies have found that increased serum L-carnitine levels can promote the development of atherosclerotic lesions.[47] The gut microbiota breaks down the serum L-carnitine into the disease-linked metabolite trimethylamine (TMA). The TMA is transported in the portal circulation to the liver, where flavin monooxygenases (FMOs) synthesize trimethylamine-N-oxidase (TMAO) from TMA. In recent years, a growing body of evidence has demonstrated a significant correlation between elevated TMAO levels and an increased risk of cardiovascular disease, as well as heightened overall mortality rates.[48]

Allicin upregulates L-Palmitoylcarnitine, a critical endogenous fatty acid metabolite that may inhibit arterial thrombosis and reduce inflammation by enhancing the enzymatic activities of plasmin and tissue plasminogen activator.[49] Therefore, after allicin intervention, the fatty acid metabolic disorder after AMI can be improved by enhancing the activity of key enzymes in fatty acid β-oxidation, thereby improving the flexibility of myocardial energy metabolism, anti-inflammation and the prognosis of AMI. Furthermore, research indicates that various phosphatidylethanolamines (PEs) species, which decrease in unstable plaques and inversely correlate with CAD severity and myocardial markers, can be restored by allicin post-AMI, implicating involvement in glycerophospholipid metabolism.[50]

The field of network pharmacology has recently experienced rapid development, being widely employed in evaluating the pharmacological value of multiple medicines in systems biology studies.[51] Therefore, to explore the protective effects and specific mechanisms of allicin against AMI, network pharmacology was used to identify potential molecular targets and pathways. PPI core genes network and pathway enrichment analysis revealed that inflammatory responses related to pyroptosis were significantly enriched, including the NF-κB signaling pathway, NLRP3 inflammasome, and signaling by Interleukins. Acute inflammatory response will occur in the body after AMI, leading to excessive release of inflammatory cytokines and influencing the prognosis.[52] Therefore, inhibiting inflammatory response is a potential strategy for AMI treatment. Recent studies have focused on pyroptosis and its vital role in the development of AMI.[53] The NLRP3/caspase-1/GSDMD pathway is the canonical pyroptosis signal pathway. NLRP3 inflammasome activation amplifies the inflammatory response and cardiac tissue injury by regulating the processing and release of IL-1β and IL-18 and causing cell death by pyroptosis.[54] Inhibitors of the NLRP3 inflammasome and blockers of IL-1β and IL-18 activity have been shown to reduce injury to the myocardium of the inflammation and preserve cardiac function.[55] NF-κB is a crucial protein regulating inflammatory response, which can regulate the transcription of target genes and induce the expression of various downstream inflammatory factors.[56] Studies have confirmed that AMI can activate NF-κB, affecting the downstream NLRP3/Caspase-1/GSDMD signaling pathway.[57] Therefore, inhibition of NF-κB-mediated NLRP3/Caspase-1/GSDMD pathway may be an effective target for anti-inflammatory therapy of AMI. After experimental

verification, we found that allicin could reduce the expression of pro-inflammatory factor IL-18 and IL-1β by inhibiting NF-κB-mediated NLRP3/Caspase-1/GSDMD pathway, highlighting its potential to mitigate myocardial injury, facilitate the resolution of inflammation, and preserve cardiac function post-AMI.

Gut microbiota and metabolites are essential for host homeostasis, with dysbiosis increasing susceptibility to numerous diseases and disorders.[58,59] Our findings suggest that host parameters correlate with changes in gut microbiota and metabolites following AMI. Notably, essential metabolites such as PE species and *L-Palmitoylcarnitine* exhibit significant negative correlations with inflammatory cytokine levels while positively correlating with cardiac function. Conversely, L-carnitine positively correlates with inflammatory cytokine levels post-AMI. Beneficial bacteria, including *g_Lactobacillus, g_Prevotella, g_Alistipes*, and *g_Limosilactobacillus*, show negative correlations with inflammatory cytokines and L-carnitine levels, whereas *g_Parasutterella* displays an opposite trend. In summary, allicin may enhance myocardial recovery and reduce inflammatory reaction post-AMI by modulating gut-heart interactions, as gut microbiota, metabolites, and host parameters exhibit significant interconnections.

Conclusions

Based on our results and other references, allicin supplementation may have beneficial effects to restore cardiac function, mitigated the progression of myocardial injury, and decreased inflammatory cytokine levels when combined with standard treatment among AMI mice. The therapeutic effect appears to be partially mediated by safeguarding the integrity of the intestinal barrier following AMI, reinstating gut microbiota and metabolites homeostasis, and regulating key enzymes involved in fatty acid metabolic pathways to enhance energy metabolism flexibility. Mechanistically, allicin suppressed pyroptosis by inhibiting the NF-κB-mediated NLRP3/Caspase-1/GSDMD pathway to reduce inflammatory response after AMI. The results of this study provide a theoretical basis and new ideas for the clinical application of allicin as a dietary supplement and adjuvant therapy to improve the prognosis of AMI.

Abbreviations

ACS, Acute coronary syndrome; AMI, Acute myocardial infarction; ATP, Adenosine triphosphate; BMI, Body Mass Index; CACT, Carnitine/acylcarnitine translocase; CoA, Acyl-coenzyme A; CPT1, Carnitine palmitoyl transferase 1; CVD, Cardiovascular disease; EF, Ejection fraction; ELISA, Enzyme-linked immunosorbent assay; FS, Fractional shortening; HE, Hematoxylin and eosin; HF, Heart failure; IL-18, Interleukin-18; IL-1β, Interleukin-1β; LAD, Left anterior descending coronary artery; LV, Left ventricular; LVIDd, Left ventricular internal end-diastolic diameter; LVIDs, Left ventricular internal end-systolic diameter; PCI, Percutaneous coronary intervention; PE, Phosphatidylethanolamine; PCoA, Principal Coordinate Analysis; SBP, Systolic blood pressure; STEMI, ST-elevation myocardial infarction; MACE, Major adverse cardiovascular events; NP, Network pharmacology; ZO-1, Zonula occludens-1.

Data Sharing Statement

The datasets used during the current study are available from the corresponding author on reasonable request. The use of database data in this study was reviewed and approved for implementation by the Clinical Research Institute of China-Japan Friendship Hospital.

Ethics Statement

The animal study was conducted in strict adherence to the guidelines for the care and use of laboratory animals, as set forth by the US National Institutes of Health (NIH Publication No. 8023, revised 1978), and received approval from the Animal Ethics Committee of the Clinical Research Institute of China-Japan Friendship Hospital (approval number: zryhyy61-03-56).

Author Contributions

All authors made a significant contribution to the work reported, whether that is in the conception, study design, execution, acquisition of data, analysis and interpretation, or in all these areas; took part in drafting, revising, or critically

reviewing the article; gave final approval of the version to be published; have agreed on the journal to which the article has been submitted; and agree to be accountable for all aspects of the work.

Funding

This research was funded by the National Natural Science Foundation of China, grant number 82274331.

Disclosure

The authors declare no conflicts of interest in this work.

References

1. Virani SS, Alonso A, Aparicio HJ, et al. Heart disease and stroke statistics-2021 update: a report from the American heart association. *Circulation*. 2021;143(8):e254–e743. doi:10.1161/CIR.0000000000000950
2. Galli M, Niccoli G, De Maria G, et al. Coronary microvascular obstruction and dysfunction in patients with acute myocardial infarction. *Nat Rev Cardiol*. 2024;21(5):283–298. doi:10.1038/s41569-023-00953-4
3. Tang WH, Kitai T, Hazen SL. Gut microbiota in cardiovascular health and disease. *Circ Res*. 2017;120(7):1183–1196. doi:10.1161/CIRCRESAHA.117.309715
4. Tousoulis D, Guzik T, Padro T, et al. Mechanisms, therapeutic implications, and methodological challenges of gut microbiota and cardiovascular diseases: a position paper by the ESC working group on coronary pathophysiology and microcirculation. *Cardiovasc Res*. 2022;118(16):3171–3182. doi:10.1093/cvr/cvac057
5. Zhou B, Wang Z, Dou Q, et al. Long-term outcomes of esophageal and gastric cancer patients with cardiovascular and metabolic diseases: a two-center propensity score-matched cohort study. *J Transl Int Med*. 2023;11(3):234–245. doi:10.2478/jtim-2023-0112
6. Lam V, Su J, Hsu A, Gross GJ, Salzman NH, Baker JE. Intestinal microbial metabolites are linked to severity of myocardial infarction in rats. *PLoS One*. 2016;11(8):e0160840. doi:10.1371/journal.pone.0160840
7. Lam V, Su J, Koprowski S, et al. Intestinal microbiota determine severity of myocardial infarction in rats. *FASEB j*. 2012;26(4):1727–1735. doi:10.1096/fj.11-197921
8. Zhou X, Li J, Guo J, et al. Gut-dependent microbial translocation induces inflammation and cardiovascular events after ST-elevation myocardial infarction. *Microbiome*. 2018;6(1):66. doi:10.1186/s40168-018-0441-4
9. Desai MS, Seekatz AM, Koropatkin NM, et al. A dietary fiber-deprived gut microbiota degrades the colonic mucus barrier and enhances pathogen susceptibility. *Cell*. 2016;167(5):1339–53.e21. doi:10.1016/j.cell.2016.10.043
10. Marques FZ, Nelson E, Chu PY, et al. High-fiber diet and acetate supplementation change the gut microbiota and prevent the development of hypertension and heart failure in hypertensive mice. *Circulation*. 2017;135(10):964–977. doi:10.1161/CIRCULATIONAHA.116.024545
11. Li S, Guo W, Lau W, et al. The association of garlic intake and cardiovascular risk factors: a systematic review and meta-analysis. *Crit Rev Food Sci Nutr*. 2023;63(26):8013–8031. doi:10.1080/10408398.2022.2053657
12. Chen K, Xie K, Liu Z, et al. Preventive effects and mechanisms of garlic on dyslipidemia and gut microbiome dysbiosis. *Nutrients*. 2019;11(6):1225. doi:10.3390/nu11061225
13. Schwingshackl L, Missbach B, Hoffmann G. An umbrella review of garlic intake and risk of cardiovascular disease. *Phytomedicine*. 2016;23(11):1127–1133. doi:10.1016/j.phymed.2015.10.015
14. Xu S, Liao Y, Wang Q, Liu L, Yang W. Current studies and potential future research directions on biological effects and related mechanisms of allicin. *Crit Rev Food Sci Nutr*. 2023;63(25):7722–7748. doi:10.1080/10408398.2022.2049691
15. Tudu CK, Dutta T, Ghorai M, et al. Traditional uses, phytochemistry, pharmacology and toxicology of garlic (Allium sativum), a storehouse of diverse phytochemicals: a review of research from the last decade focusing on health and nutritional implications. *Front Nutr*. 2022;9:949554. doi:10.3389/fnut.2022.929554
16. Lu M, Pan J, Hu Y, et al. Advances in the study of vascular related protective effect of garlic (Allium sativum) extract and compounds. *J Nutr Biochem*. 2024;124:109531. doi:10.1016/j.jnutbio.2023.109531
17. Cui T, Liu W, Yu C, et al. Protective effects of allicin on acute myocardial infarction in rats via hydrogen sulfide-mediated regulation of coronary arterial vasomotor function and myocardial calcium transport. *Front Pharmacol*. 2021;12:752244. doi:10.3389/fphar.2021.752244
18. Xu W, Li XP, Li EZ, et al. Protective effects of allicin on ISO-induced rat model of myocardial infarction via JNK signaling pathway. *Pharmacology*. 2020;105(9–10):505–513. doi:10.1159/000503755
19. Liu Z, Huang Y, Li H, et al. A generalized deep learning model for heart failure diagnosis using dynamic and static ultrasound. *J Transl Int Med*. 2023;11(2):138–144. doi:10.2478/jtim-2023-0088
20. Peterzan MA, Lygate CA, Neubauer S, Rider OJ. Metabolic remodeling in hypertrophied and failing myocardium: a review. *Am j Physiol Heart Circulatory Physiol*. 2017;313(3):H597–h616. doi:10.1152/ajpheart.00731.2016
21. Lopaschuk GD, Karwi QG, Tian R, Wende AR, Abel ED. Cardiac energy metabolism in heart failure. *Circ res*. 2021;128(10):1487–1513. doi:10.1161/CIRCRESAHA.121.318241
22. Ridker PM, MacFadyen JG, Thuren T, Libby P. Residual inflammatory risk associated with interleukin-18 and interleukin-6 after successful interleukin-1β inhibition with canakinumab: further rationale for the development of targeted anti-cytokine therapies for the treatment of atherothrombosis. *Eur Heart J*. 2020;41(23):2153–2163. doi:10.1093/eurheartj/ehz542
23. Mak'Anyengo R, Duewell P, Reichl C, et al. Nlrp3-dependent IL-1β inhibits CD103+ dendritic cell differentiation in the gut. *JCI Insight*. 2018;3(5). doi:10.1172/jci.insight.96322
24. van der Bijl P, Abou R, Goedemans L, et al. Left ventricular post-infarct remodeling: implications for systolic function improvement and outcomes in the modern era. *JACC Heart Fail*. 2020;8(2):131–140. doi:10.1016/j.jchf.2019.08.014

25. Belli M, Barone L, Longo S, et al. Gut microbiota composition and cardiovascular disease: a potential new therapeutic target? *Int J mol Sci*. 2023;24(15):11971. doi:10.3390/ijms241511971
26. Sánchez-Gloria JL, Arellano-Buendía AS, Juárez-Rojas JG, et al. Cellular mechanisms underlying the cardioprotective role of allicin on cardiovascular diseases. *Int J mol Sci*. 2022;23(16):9082. doi:10.3390/ijms23169082
27. Liu S, He L, Jiang Q, et al. Effect of dietary α-ketoglutarate and allicin supplementation on the composition and diversity of the cecal microbial community in growing pigs. *J Sci Food Agric*. 2018;98(15):5816–5821. doi:10.1002/jsfa.9131
28. Zhang C, He X, Sheng Y, et al. Allicin-induced host-gut microbe interactions improves energy homeostasis. *FASEB j*. 2020;34(8):10682–10698. doi:10.1096/fj.202001007R
29. Ettehad-Marvasti F, Ejtahed HS, Siadat SD, et al. Effect of garlic extract on weight loss and gut microbiota composition in obese women: a double-blind randomized controlled trial. *Front Nutr*. 2022;9:1007506. doi:10.3389/fnut.2022.1007506
30. Panyod S, Wu WK, Chen PC, et al. Atherosclerosis amelioration by allicin in raw garlic through gut microbiota and trimethylamine-N-oxide modulation. *NPJ Biofilms Microbiomes*. 2022;8(1):4. doi:10.1038/s41522-022-00266-3
31. Zhao J, Zhang Q, Cheng W, et al. Heart-gut microbiota communication determines the severity of cardiac injury after myocardial ischaemia/reperfusion. *Cardiovasc Res*. 2023;119(6):1390–1402. doi:10.1093/cvr/cvad023
32. Hu P, Yuan M, Guo B, et al. Citric acid promotes immune function by modulating the intestinal barrier. *Int J mol Sci*. 2024;25(2):1239.
33. Stojanov S, Berlec A, Štrukelj B. The influence of probiotics on the Firmicutes/Bacteroidetes ratio in the treatment of obesity and inflammatory bowel disease. *Microorganisms*. 2020;8(11). doi:10.3390/microorganisms8111715
34. Liu M, Wang M, Peng T, et al. Gut-microbiome-based predictive model for ST-elevation myocardial infarction in young male patients. *Front Microbiol*. 2022;13:1031878. doi:10.3389/fmicb.2022.1031878
35. Zhang Z, Cai B, Sun Y, Deng H, Wang H, Qiao Z. Alteration of the gut microbiota and metabolite phenylacetylglutamine in patients with severe chronic heart failure. *Front Cardiovasc Med*. 2022;9:1076806. doi:10.3389/fcvm.2022.1076806
36. Palmu J, Börschel CS, Ortega-Alonso A, et al. Gut microbiome and atrial fibrillation-results from a large population-based study. *EBioMedicine*. 2023;91:104583. doi:10.1016/j.ebiom.2023.104583
37. Gomez-Arango LF, Barrett HL, McIntyre HD, Callaway LK, Morrison M, Dekker Nitert M. Increased systolic and diastolic blood pressure is associated with altered gut microbiota composition and butyrate production in early pregnancy. *Hypertension*. 2016;68(4):974–981. doi:10.1161/HYPERTENSIONAHA.116.07910
38. Zhao X, Zhong X, Liu X, Wang X, Gao X. Therapeutic and improving function of lactobacilli in the prevention and treatment of cardiovascular-related diseases: a novel perspective from gut microbiota. *Front Nutr*. 2021;8:693412. doi:10.3389/fnut.2021.693412
39. Gao J, Yan KT, Wang JX, et al. Gut microbial taxa as potential predictive biomarkers for acute coronary syndrome and post-STEMI cardiovascular events. *Sci Rep*. 2020;10(1):2639. doi:10.1038/s41598-020-59235-5
40. Cai JJ, Liu Y, Wang J, et al. Lactobacillus levels and prognosis of patients with acute myocardial infarction. *J Geriatr Cardiol*. 2022;19(2):101–114. doi:10.11909/j.issn.1671-5411.2022.02.009
41. Liu TT, Wang J, Liang Y, et al. The level of serum total bile acid is related to atherosclerotic lesions, prognosis and gut Lactobacillus in acute coronary syndrome patients. *Ann Med*. 2023;55(1):2232369. doi:10.1080/07853890.2023.2232369
42. Tannahill GM, Curtis AM, Adamik J, et al. Succinate is an inflammatory signal that induces IL-1β through HIF-1α. *Nature*. 2013;496(7444):238–242. doi:10.1038/nature11986
43. Gutiérrez-Calabrés E, Ortega-Hernández A, Modrego J, et al. Gut microbiota profile identifies transition from compensated cardiac hypertrophy to heart failure in hypertensive rats. *Hypertension*. 2020;76(5):1545–1554. doi:10.1161/HYPERTENSIONAHA.120.15123
44. Lopaschuk GD, Ussher JR, Folmes CD, Jaswal JS, Stanley WC. Myocardial fatty acid metabolism in health and disease. *Physiol Rev*. 2010;90(1):207–258. doi:10.1152/physrev.00015.2009
45. Schlaepfer IR, Joshi M. CPT1A-mediated fat oxidation, mechanisms, and therapeutic potential. *Endocrinology*. 2020;161(2). doi:10.1210/endocr/bqz046
46. Elantary R, Othman S. Role of L-carnitine in cardiovascular health: literature review. *Cureus*. 2024;16(9):e70279. doi:10.7759/cureus.70279
47. Koeth RA, Wang Z, Levison BS, et al. Intestinal microbiota metabolism of L-carnitine, a nutrient in red meat, promotes atherosclerosis. *Nat Med*. 2013;19(5):576–585. doi:10.1038/nm.3145
48. Li XS, Obeid S, Klingenberg R, et al. Gut microbiota-dependent trimethylamine N-oxide in acute coronary syndromes: a prognostic marker for incident cardiovascular events beyond traditional risk factors. *Eur Heart J*. 2017;38(11):814–824. doi:10.1093/eurheartj/ehw582
49. Yang J, Cha L, Wang Y, et al. L-Palmitoylcarnitine potentiates plasmin and tPA to inhibit thrombosis. *Nat Prod Bioprospect*. 2023;13(1):48. doi:10.1007/s13659-023-00413-z
50. Chen H, Wang Z, Qin M, et al. Comprehensive metabolomics identified the prominent role of glycerophospholipid metabolism in coronary artery disease progression. *Front Mol Biosci*. 2021;8:632950. doi:10.3389/fmolb.2021.632950
51. Nogales C, Mamdouh ZM, List M, Kiel C, Casas AI, Schmidt H. Network pharmacology: curing causal mechanisms instead of treating symptoms. *Trends Pharmacol Sci*. 2022;43(2):136–150. doi:10.1016/j.tips.2021.11.004
52. Ong SB, Hernández-Reséndiz S, Crespo-Avilan GE, et al. Inflammation following acute myocardial infarction: multiple players, dynamic roles, and novel therapeutic opportunities. *Pharmacol Ther*. 2018;186:73–87. doi:10.1016/j.pharmthera.2018.01.001
53. Toldo S, Abbate A. The role of the NLRP3 inflammasome and pyroptosis in cardiovascular diseases. *Nat Rev Cardiol*. 2024;21(4):219–237. doi:10.1038/s41569-023-00946-3
54. Liu W, Shen J, Li Y, et al. Pyroptosis inhibition improves the symptom of acute myocardial infarction. *Cell Death Dis*. 2021;12(10):852. doi:10.1038/s41419-021-04143-3
55. Toldo S, Mezzaroma E, Buckley LF, et al. Targeting the NLRP3 inflammasome in cardiovascular diseases. *Pharmacol Ther*. 2022;236:108053. doi:10.1016/j.pharmthera.2021.108053
56. Jaén RI, Val-Blasco A, Prieto P, et al. Innate immune receptors, key actors in cardiovascular diseases. *JACC Basic Transl Sci*. 2020;5(7):735–749. doi:10.1016/j.jacbts.2020.03.015
57. Hua F, Li JY, Zhang M, et al. Kaempferol-3-O-rutinoside exerts cardioprotective effects through NF-κB/NLRP3/Caspase-1 pathway in ventricular remodeling after acute myocardial infarction. *J Food Biochem*. 2022;46(10):e14305. doi:10.1111/jfbc.14305

58. Hays KE, Pfaffinger JM, Ryznar R. The interplay between gut microbiota, short-chain fatty acids, and implications for host health and disease. *Gut Microbes*. 2024;16(1):2393270. doi:10.1080/19490976.2024.2393270
59. Wang W, Fan Z, Yan Q, et al. Gut microbiota determines the fate of dietary fiber-targeted interventions in host health. *Gut Microbes*. 2024;16(1):2416915. doi:10.1080/19490976.2024.2416915